RESEARCH ARTICLE

MAGINAV: Long-Term Accurate Navigation Algorithm Using Inertial and Magnetic Field Sensor Fusion

KONSTANTINOS PAPAFOTIS, (Member, IEEE), AND PAUL P. SOTIRIADIS, (Fellow, IEEE)

Department of Electrical and Computer Engineering, National Technical University of Athens, 15780 Athens, Greece

Corresponding author: Konstantinos Papafotis (kpapafotis@mail.ntua.gr)

ABSTRACT MAGINAV (MAGnetic Inertial NAVigation) algorithm provides accurate estimation of velocity, attitude and position in long-term. It is utilized in a specialized pedestrian navigation system that consists of a three-axis accelerometer, a three-axis gyroscope, and a three-axis magnetometer mounted on the shoe of a walking human. MAGINAV compensates for the attitude error, accumulated over time by using a second attitude estimation obtained by fusing the measurements of the accelerometer and the magnetometer Instead of employing a complex Attitude Heading Reference System (AHRS), MAGINAV utilizes the computationally efficient TRIAD algorithm, alongside two popular algorithms for zero-velocity detection and magnetic-disturbance detection respectively. The proposed algorithm undergoes testing in an outdoor environment using low-cost commercial inertial and magnetic field sensors. Remarkably, it achieves exceptional long-term accuracy, with a position error that is less than 0.25% of the total distance in a 20-minute walk spanning $1.3km$.

I. INTRODUCTION

Satellite-based navigation systems (GPS,GLONASS etc.) have established their dominance in the field. These systems come in different grades, offering varying levels of accuracy to suit diverse applications, ranging from low-cost commercial implementations to high-end industrial and military ones. However, despite the quality of high-end systems, all satellite navigation technologies share inherent drawbacks. They exhibit limited refresh rates, are ineffective in indoor environments, and are vulnerable to jamming. In response to these limitations, alternative navigation technologies have emerged over the past few decades.

Inertial navigation systems (INS) utilize inertial sensors, namely accelerometers and gyroscopes, to calculate the attitude, velocity, and position of moving objects. Initially

developed for rocket guidance during World War II, they have found widespread use in marine, aerospace, military, and even commercial applications. The advent of micro-electro-mechanical (MEM) inertial sensors in recent years has further expanded their usage. With their small size and low cost, MEM inertial sensors have been integrated into numerous consumer devices like smartphones and activity trackers contributing to the growth of inertial navigation applications.

Pedestrian navigation, specifically using inertial sensors, has gained significant attention in recent years. Many studies have employed miniature inertial sensors mounted on the human body and proposed various algorithms to estimate the individual's attitude, velocity, and position [1], [2], [3], [4], [5], [6], [7], [8], [9], [10], [11], [12], [13], [14]. A key aspect of designing such systems revolves around compensating for the substantial error characteristics inherent in inertial sensors [15], [16].

The associate editor coordinating the review of this manuscript and approving it for publication was Agustin Leobardo Herrera-May.

Most pedestrian inertial navigation systems employ shoe-mounted inertial sensors and the zero velocity update method to improve the accuracy of attitude, velocity, and position estimates [1], [2], [3], [6], [9]. Specifically, these systems utilize a zero velocity detection algorithm to identify the stance phase of human walking, during which the velocity of the shoe is zero. This information is then used to estimate the velocity, attitude, and position errors, typically through a Kalman filter.

While the zero velocity update method yields accurate results over short time periods, the use of low-cost sensors can lead to accumulated errors over time, significantly degrading long-term navigation accuracy. The dominant source of position error arises from attitude errors caused by gyroscope noise, offset drift, and residual calibration errors [15].

For applications where cost is not a concern, expensive, factory-calibrated gyroscopes are used to minimize attitude errors. However, in commercial applications where cost is a critical factor, a popular approach involves combining the zero velocity update method with an Attitude Heading Reference (AHR) algorithm. Typically, these algorithms utilize measurements from a three-axis magnetometer to derive an accurate long-term attitude estimate. Several different AHR algorithms have been proposed [14], [17], [18], [19], [20], [21], [22], [23], employing estimation [21], [22], [23], optimization [18], or filtering [17], [19] techniques. Despite the significant improvement in attitude estimation offered by existing AHR algorithms, their computational complexity poses challenges for applications with limited computational power.

This paper presents MAGINAV [24], a computationally efficient pedestrian navigation algorithm that offers long-term accuracy using inertial and magnetic field sensors. Specifically, MAGINAV utilizes a three-axis accelerometer, a three-axis gyroscope, and a three-axis magnetometer mounted on the shoe of a walking human to estimate their velocity, attitude, and position. The algorithm is based on the widely adopted zero velocity update method and introduces a computationally efficient attitude estimation scheme utilizing the TRIAD algorithm and measurements from both the accelerometer and the magnetometer.

The performance evaluation of the MAGINAV algorithm is done by using low-cost MEM inertial and magnetic field sensors. The sensors were calibrated and their sensitivity axes were aligned using the MAG.I.C.AL. methodology [25], requiring no specialized equipment. The algorithm's accuracy and efficiency were assessed through a 20-minute, 1.3km walk in a suburban environment. The performance of MAGINAV was compared to similar algorithms based on two popular and highly cited AHR systems. Notably, MAGINAV achieved an extremely small position error, accounting for less than 0.2% of the total distance walked.

The remainder of this paper is structured as follows. Section II provides a detailed presentation and analysis of the proposed system. The experimental setup, along with the performance evaluation of the proposed system, is presented in Section III. Finally, Section IV draws the conclusions of the study.

II. THE PROPOSED INERTIAL NAVIGATION SYSTEM

This section presents the proposed pedestrian inertial navigation system and provides a detailed analysis of each functional block. The following notation is used throughout the paper and is introduced first.

A. NOTATION AND ASSUMPTIONS

Different notations have been used in the literature to describe basic kinematic quantities such as velocity, acceleration, and position. In this work, we adopt the notation from [16], where a kinematic quantity x is denoted as $x_{\beta\alpha}^{\gamma}$, with α representing the object frame, β representing the reference frame, and γ denoting the resolving frame.

When referring to the measurement of an inertial or magnetic sensor, the object frame and the reference frame are fixed and correspond to the sensor's coordinate frame and the inertial frame, respectively. For simplicity, a measurement is denoted as y_{γ}.

The orthogonal, frame transformation matrix, transforming the resolving frame of a kinematic quantity from α to β, is denoted as C_{α}^{β}.

The Cross Product Matrix of a vector $x = \begin{bmatrix} x_1 & x_2 & x_3 \end{bmatrix}^T$, is defined as [26]

$$[x \times] = \begin{bmatrix} 0 & -x_3 & x_2 \\ x_3 & 0 & -x_1 \\ -x_2 & x_1 & 0 \end{bmatrix}$$

The notation used in the rest of this work is summarized in Table 1. Additionally, the following assumptions are made:

1) The three sensors are fixed on the same rigid platform, which is mounted on the shoe of a walking person.
2) Each sensor is individually calibrated, and their sensitivity axes are aligned.
3) The three sensors are sampled simultaneously with a common, constant sampling rate τ_s.
4) At the start of the experiment, the sensor platform is stationary and free from magnetic disturbance.

B. TOP-LEVEL SYSTEM ARCHITECTURE

The architecture of the proposed inertial navigation system is depicted in Figure 1. This system utilizes measurements from a three-axis accelerometer, denoted as f_b, a three-axis gyroscope, denoted as ω_b, and a three-axis magnetometer, denoted as m_b, to estimate the velocity v, position p and attitude C of a walking human.

For each sensor measurement, the system obtains an initial attitude estimate C_K using the gyroscope measurement. To correct the accumulated attitude error over the long term, the system employs a second independent attitude estimate derived from the accelerometer and magnetometer

TABLE 1. Notation.

Coordinate Frames	
b	sensors' platform (body) frame
i	inertial frame
Kinematic Quantities	
$f^{\gamma}_{\beta\alpha} : \mathbb{R} \to \mathbb{R}^3$	specific force
$\omega^{\gamma}_{\beta\alpha} : \mathbb{R} \to \mathbb{R}^3$	angular velocity
$v^{\gamma}_{\beta\alpha} : \mathbb{R} \to \mathbb{R}^3$	velocity
$p^{\gamma}_{\beta\alpha} : \mathbb{R} \to \mathbb{R}^3$	position
$C^i_b : \mathbb{R} \to SO(3)$	attitude
Sensors' Measurements	
$f_{\gamma} : \mathbb{Z} \to \mathbb{R}^3$	accelerometer's measurement
$\omega_{\gamma} : \mathbb{Z} \to \mathbb{R}^3$	gyroscope's measurement
$m_{\gamma} : \mathbb{Z} \to \mathbb{R}^3$	magnetometer's measurement
$\tau_s \in \mathbb{R}$	sensors' sampling period
System's Outputs	
$v : \mathbb{Z} \to \mathbb{R}^3$	velocity output
$p : \mathbb{Z} \to \mathbb{R}^3$	position output
$C : \mathbb{Z} \to SO(3)$	attitude output
Other Notation	
$I_n \in SO(3)$	$n \times n$ identity matrix
$O_n \in \mathbb{R}^3$	$n \times n$ matrix of zeros
$\|\cdot\|$	Euclidean norm

measurements. This is achieved by applying the TRIAD algorithm when a zero velocity condition ($ZV = 1$ in Figure 1) is detected and there is no magnetic disturbance ($D = 1$ in Figure 1). The resulting second attitude estimate is denoted as C_{FM}, and it updates the attitude estimate C_{GFM} accordingly (see Figure 1).

The next step involves deriving an initial velocity estimate v_K and position estimate p_K. This is accomplished by utilizing the corrected attitude C_{GFM} along with the accelerometer measurement and applying the kinematic equations.

Finally, the zero velocity update method is employed to further enhance the velocity, attitude, and position estimates. This method is implemented using a Kalman filter and is applied whenever a zero velocity condition is detected ($ZV = 1$ in Figure 1).

C. ZERO VELOCITY DETECTION

The zero velocity detection algorithm plays a crucial role in pedestrian navigation systems that utilize shoe-mounted sensors as part of the widely adopted zero velocity update method. In the proposed system, the zero velocity information is utilized for implementing the zero velocity update method (see Section II-I) and deriving a long-term accurate attitude estimate using measurements from the magnetometer and accelerometer (see Section II-F).

Zero velocity detection algorithms utilize data from inertial sensors along with information about the human walking pattern to detect the stance phase of walking [2], [6], [27], [28]. More advanced algorithms incorporate

additional sensors, such as pressure sensors, to enhance the accuracy of zero velocity detection [4]. Various review papers compare the performance characteristics of existing zero velocity detection algorithms [2], [27]. In practical navigation scenarios, different zero velocity detection algorithms tend to exhibit similar performance [2].

In our system, we employ the accelerometer measurement f_b and the gyroscope measurement ω_b to detect zero velocity based on the algorithm introduced in [27].

The first step involves calculating the mean value of the accelerometer measurements $\bar{f_b}(k)$ using a rolling window of size N:

$$f_b\bar{(k)} = \frac{1}{N} \sum_{k}^{(k+N-1)} f_b(k) \tag{1}$$

To determine if a zero velocity condition is present at time k, we compute the quantity:

$$T(k) = \sum_{k}^{(k+N-1)} \left(\frac{1}{\sigma_a^2} \left\| f_b(k) - g \frac{\bar{f_b}(k)}{\|\bar{f_b}(k)\|} \right\|^2 + \frac{1}{\sigma_g^2} \|\omega_b(k)\|^2 \right) \tag{2}$$

where σ_a^2 and σ_g^2 are the noise variances of the accelerometer and gyroscope, respectively, and g is the gravitational acceleration.

According to [27], we define:

$$ZV(k) = \begin{cases} 1, & T(k) < \gamma_z \\ 0, & \text{otherwise} \end{cases} \tag{3}$$

where γ_z is a threshold parameter. In (3), $ZV(k) = 1$ indicates the existence of a zero velocity condition.

Special attention should be given to parameterizing the zero velocity detection algorithm. The error variances σ_a^2 and σ_g^2, as well as the threshold value γ_z, used by the algorithm to determine the zero velocity condition must be carefully selected and fine-tuned to achieve optimal performance.

D. MAGNETIC DISTURBANCE DETECTION

To perform attitude determination using the accelerometer and magnetometer measurements via the TRIAD algorithm, it is necessary for both sensors to remain stationary and free from magnetic disturbance. The stillness condition is met during the stance phase of human walking when the shoe makes contact with the ground. On the other hand, identifying magnetic disturbances is more challenging as they can unpredictably distort the Earth's magnetic field.

In this work, we utilize the magnitude of the measured magnetic field, denoted as m_b, to detect magnetic disturbances. We exploit the fact that in the absence of magnetic disturbance, the magnitude of the measured magnetic field, m_b, should be equal to that of the Earth's magnetic field, m_{earth}. Assuming that the magnetometer is placed away from magnetic disturbances when the experiment begins,
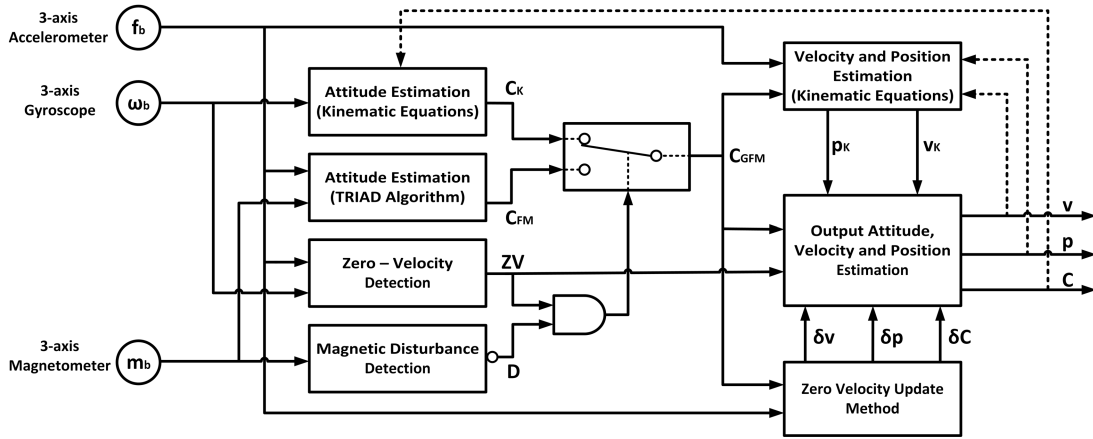
FIGURE 1. Architecture of the proposed pedestrian inertial navigation system.

and considering the sensor's noise and measurement errors, we can express this relationship as:

$$\|m_{\text{earth}}\| \approx \|m_b(0)\| \tag{4}$$

To determine the presence of magnetic disturbance, we introduce a tolerance parameter m_{thr}. We define:

$$D(k) = \begin{cases} 0, & \|\|m_{\text{earth}}\| - \|m_b(k)\|\| > m_{\text{thr}} \\ 1, & \text{otherwise} \end{cases} \tag{5}$$

If the difference between the magnitudes exceeds the threshold value m_{thr}, we have $D(k) = 0$, indicating the presence of magnetic disturbance. Conversely, if no magnetic disturbance is detected, we have $D(k) = 1$.

E. ATTITUDE ESTIMATION USING KINEMATIC EQUATIONS AND GYROSCOPE MEASUREMENTS

The standard kinematic equations are employed to obtain an initial estimate of the attitude of the sensors' platform. We begin by calculating the attitude at time t, denoted as $C_b^i(t) \in SO(3)$. To achieve this, we can express [16]:

$$\dot{C}_b^i(t) = C_b^i(t)[\omega_{ib}^b(t) \times] \tag{6}$$

Based on (6) and assuming that the angular velocity of the platform remains constant during the short time period between consecutive samples, $[t, t + \tau_s]$, we have:

$$C_b^i(t + \tau_s) = C_b^i(t)\exp\left([\omega_{ib}^b(t) \times]\tau_s\right) \tag{7}$$

Using (7), we can approximate the attitude at time $k\tau_s$ based on the gyroscope measurement $\omega_b(k)$:

$$C_b^i(k\tau_s) \approx C_b^i((k-1)\tau_s)(I_3 + [\omega_b(k) \times]\tau_s) \tag{8}$$

Equation (8) implies that the estimated attitude at time $k\tau_s$, denoted as $C_b^i(k\tau_s)$, is influenced by the accumulated noise from all previous gyroscope measurements. In the proposed system, we utilize the output attitude $C(k-1)$ as feedback to reset the accumulated error when a more accurate attitude estimate becomes available (either from the zero velocity

update method or the TRIAD algorithm). Hence, according to (8), we define:

$$C_K(k) \triangleq C(k-1)(I_3 + [\omega_b(k) \times]\tau_s) \tag{9}$$

F. ATTITUDE ESTIMATION USING THE TRIAD ALGORITHM, AND ACCELEROMETER AND MAGNETOMETER MEASUREMENTS

In INS, attitude is commonly calculated using the gyroscope and equation (9), or a different approximation of (7). However, this approach leads to the accumulation of attitude errors which is significant in the long term. In this section, we utilize the TRIAD algorithm [29], [30] to calculate a second estimate of the attitude using the accelerometer's and the magnetometer's measurements.

Let a_1, a_2, b_1, and b_2 be four 3×1 unit vectors, and let R be a matrix in $SO(3)$ such that $a_2 = Ra_1$ and $b_2 = Rb_1$. Given these four vectors as inputs, the TRIAD algorithm derives R. It is convenient to consider the TRIAD algorithm as a function of the four vectors, i.e.:

$$R = \text{TRIAD}(a_1, b_1, a_2, b_2) \tag{10}$$

A more detailed description of the TRIAD algorithm is given in Appendix A.

Now, consider the measurements of the accelerometer, $f_b(k_c)$, and the magnetometer, $f_b(k_c)$, at discrete time $k = k_c > 0$. We assume that at time k_c, the sensors are still ($ZV = 1$ in Figure 1), and no magnetic disturbance is present ($D = 1$ in Figure 1). Utilizing the measurements of these two sensors and the TRIAD algorithm, we obtain the following estimate:

$$C_{FM}(k_c) = C(0)\,\text{TRIAD}\,(f_b(0), m_b(0), f_b(k_c), m_b(k_c)) \tag{11}$$

Here, $C(0)$, $f_b(0)$, and $m_b(0)$ are captured at the beginning of the experiment when the sensors are still and free from magnetic disturbance.

G. ATTITUDE DERIVATION BY FUSING THE TWO ATTITUDE ESTIMATES AND THE ZERO-VELOCITY UPDATE

The attitude, C, is calculated using the attitude estimates C_K and C_{FM} in combination with the correction term, δC. The operation of the proposed algorithm can be divided into 3 states, as shown in Table 2, based on the results of the zero velocity detection ZV, and the magnetic disturbance detection, D, algorithms.

TABLE 2. Operation states.

	D = 0	**D = 1**
ZV = 0	State 1	
ZV = 1	State 2	State 3

In State 1, the attitude is derived using the kinematics equations and (9). During State 2, the zero velocity update method is utilized to compensate for gyroscope measurement errors. Finally, in State 3, the measurements of the accelerometer and the magnetometer are used to derive an accurate estimation of the attitude using the TRIAD algorithm. Thus, the attitude C, for each operation state is as follows:

$$C(k) = \begin{cases} C_K(k), & \text{State 1} \\ \delta C\, C_K(k), & \text{State 2} \\ C_{FM}, & \text{State 3} \end{cases} \tag{12}$$

H. VELOCITY AND POSITION ESTIMATION USING KINEMATIC EQUATIONS AND ACCELEROMETER MEASUREMENTS

To obtain an initial estimate of the velocity and position, we define the intermediate attitude C_{GFM} according to Figure 1 as follows:

$$C_{GFM}(k) = \begin{cases} C_{FM}(k), & \text{if } ZV = 1 \text{ and } D = 1 \\ C_K(k), & \text{otherwise} \end{cases} \tag{13}$$

Next, we transform the accelerometer's measurement (naturally expressed in the sensors' platform frame) to the inertial frame using $C_{GFM}(k)$:

$$f_i(k) = C_{GFM}(k)f_b(k) \tag{14}$$

We eliminate the effect of gravity acceleration on the accelerometer measurement, by defining:

$$a(k) = f_i(k) + g_i \tag{15}$$

where g_i represents the 3×1 gravitational acceleration vector expressed in the inertial frame. The discrete-time position and velocity vectors are calculated as follows:

$$v_K(k) = v_K(k-1) + a(k)\tau_s \tag{16}$$

$$p_K(k) = p_K(k-1) + \frac{1}{2}(v_K(k) + v_K(k-1))\tau_s \tag{17}$$

I. ZERO VELOCITY UPDATE METHOD

The zero velocity update method is utilized by a Kalman filter, similar to the one presented in [16]. This filter utilizes the measurements from the accelerometer and gyroscope to estimate the errors in velocity, attitude, and position, as well as the offset of the two sensors.

In [16], the author employs a 15×1 Kalman filter state vector, denoted as x_{zv}, defined as follows:

$$x_{zv} = \begin{bmatrix} \delta\psi^T & \delta v^T & \delta p^T & b_a^T & b_g^T \end{bmatrix}^T \tag{18}$$

Here, $\delta\psi$ represents the 3×1 attitude error in Euler angles, δv is the 3×1 velocity error, δr is the 3×1 position error, b_a denotes the 3×1 accelerometer offset vector, and b_g represents the 3×1 gyroscope offset vector. By employing the kinematic equations and assuming small errors in the accelerometer and gyroscope measurements, we obtain the following state propagation model for the Kalman filter, similar to [16]:

$$x_{zv}(k+1) = \Phi_{zv}(k)x_{zv}(k) + w_{zv}(k) \tag{19}$$

In Equation (19), w_{zv} is assumed to be a white noise sequence, and $\Phi_{zv}(k)$ is given by:

$$\Phi_{zv}(k) = \begin{bmatrix} I_3 & 0_3 & 0_3 & 0_3 & C_{\tau_s}(k) \\ F(k) & I_3 & 0_3 & C_{\tau_s}(k) & 0_3 \\ 0_3 & I_3\tau_s & I_3 & 0_3 & 0_3 \\ 0_3 & 0_3 & 0_3 & I_3 & 0_3 \\ 0_3 & 0_3 & 0_3 & 0_3 & I_3 \end{bmatrix} \tag{20}$$

In Equation (20), $F(k)$ is defined as $[-f_i(k) \times]\tau_s$, and $C_{\tau_s}(k) = C_{GFM}(k)\tau_s$.

When a zero velocity condition is detected, the velocity output of the kinematic equations (as described in Section II-H) should ideally be zero. However, due to sensor imperfections, a small velocity error persists even when the sensors' platform is stationary. This velocity error is used as a measurement of the velocity error, denoted as δv, in the Kalman filter. Thus, the measurement equation of the filter takes the following form:

$$z_{zv}(k) = u_K(k) = H_{zv}x_{zv}(k) + v_{zv}(k) \tag{21}$$

In Equation (21), v_{zv} is a white noise sequence, and H_{zv} is defined as:

$$H_{zv} = \begin{bmatrix} 0_3 & I_3 & 0_3 & 0_3 & 0_3 \end{bmatrix}^T \tag{22}$$

It is crucial to initialize the diagonal covariance matrices Q_{zv} and R_{zv} properly to achieve high performance. Let σ_a^2 and σ_g^2 denote the variances of the accelerometer and gyroscope noise, respectively (assuming similar noise characteristics along each axis). Additionally, let σ_{ba}^2 and σ_{bg}^2 represent the variances of their offsets as they drift over time. The covariance matrix Q_{zv} is formed as follows:

$$Q_{zv} = \text{diag}\left(\begin{bmatrix} \sigma_g^2 1_{1\times 3} & \sigma_a^2 1_{1\times 3} & 0_{1\times 3} & \sigma_{ba}^2 1_{1\times 3} & \sigma_{bg}^2 1_{1\times 3} \end{bmatrix}\right)\tau_s \tag{23}$$

Similarly, the measurement covariance matrix R_{zv} is formed by assuming the variance of the velocity measurement in the presence of a zero-velocity condition, denoted as σ_v^2:

$$R_{zv} = \sigma_v^2 I_3 \tag{24}$$

Note that the attitude correction term $\delta\psi$ is expressed in Euler angles. By employing the small-angle approximation, the corresponding rotation matrix is defined as:

$$\delta C = [\delta\psi \times] \tag{25}$$

III. PERFORMANCE EVALUATION

In this section the performance of the proposed algorithm is evaluated through experimental measurements. However, since a key point of this work is the introduction of the attitude estimation scheme of Section II-G, we first analyze the long-term performance of this scheme both from a theoretical and a simulation point of view.

A. ATTITUDE ERROR

A qualitative representation of the attitude error evolution over time of the proposed estimation scheme is shown in Figure 2.

As observed, during State 1, the attitude error accumulates and grows over time. This is expected and supported by (9). Assuming a small error in the measurement $\omega_b(k)$, i.e. $\hat{\omega}_b(k) = \omega_b(k) + \delta\omega_b(k)$, we have

$$
\begin{aligned}
\hat{C}_K(k) &\triangleq C(k-1)\left(I_3 + [\hat{\omega}_b(k) \times]\tau_s\right) \\
&= C(k-1)\left\{I_3 + \left([\hat{\omega}_b(k) \times] + [\delta\omega_b(k) \times]\right)\tau_s\right\} \\
&= C_K(k) + C(k-1)[\delta\omega_b(k) \times]\tau_s
\end{aligned}
\tag{26}
$$

Thus, according to (26), in every new gyroscope's sample, a small error is added to the estimated attitude making it unreliable in long-term.

In State 2, the zero velocity update method prevents the error from further increasing by compensating for the measurement error during the zero-velocity phases of the human walking. However, this correction is insufficient to compensate for the accumulated attitude error, leading to a significant rise in the long term (as demonstrated in Section III using real sensor measurements).

In State 3, the attitude is calculated using TRIAD algorithm and remains bounded. This happens because the TRIAD algorithm relies only on the measurements of the accelerometer and the magnetometer at time k and at the beginning of the experiment. Consequently, the error of the TRIAD algorithm is related only to the momentarily measurement error of the two sensors at these particular time periods as shown in [31]. Therefore, during State 3, an accurate and independent attitude estimate is obtained.

Figure 2 illustrates that when accurate estimates of the attitude are frequently available, the attitude error does not significantly increase over time, resulting in a long-term accurate attitude estimation. In the case of pedestrian navigation, frequent attitude corrections are typically possible in
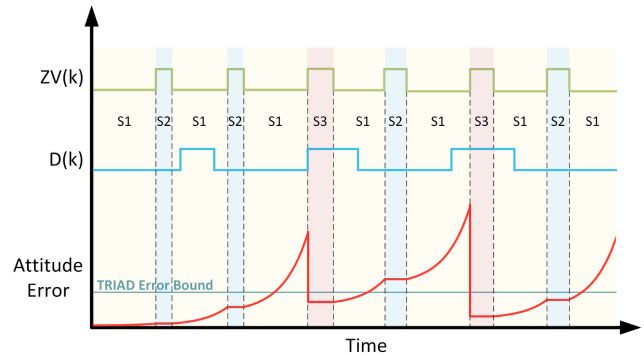

FIGURE 2. Qualitative representation of the attitude error using the introduced estimation scheme. The three operation states are denoted as S1, S2, and S3, respectively.

outdoor environment where there is no magnetic disturbance. However, even in the case of indoor environment (where building materials disturb the magnetic field) the navigation accuracy could benefit from sporadic attitude corrections when the proposed attitude estimation scheme is used.

To further demonstrate how the proposed attitude estimation scheme performs in long-term we set up a simulation in MATLAB. More specifically, we consider the measurements of a three-axis accelerometer, a three-axis gyroscope and a three-axis magnetometer attached on a still rigid object in a constant, uniform magnetic field. Ideally, the measurements of the three sensors should be constant and the object's attitude should be equal to its initial attitude. We add white noise and a small constant bias to the three sensors and simulate 5 hours of measurements. The added noise and bias levels for the three sensors are selected to match those of a typical commercial sensor (see Table 3).

In Figure 3 the attitude error (expressed in the error of the three Euler angles) when the attitude is calculated by using just the gyroscope's measurements is compared to the attitude error when the proposed method is employed and the attitude is corrected every 5 seconds using the TRIAD algorithm.[1] When just the gyroscope is used, the error rises over time leading to a large navigation errors. However, when the proposed attitude estimation scheme is used, the attitude error is small and bounded even after long time periods.

B. EXPERIMENTAL RESULTS

To evaluate the proposed inertial navigation algorithm, we utilized a low-cost LSM9DS1 system in package (SiP) by STMicroelectronics as the inertial measurement unit (IMU). The LSM9DS1 SiP consists of a three-axis accelerometer, a three-axis gyroscope, and a three-axis magnetometer. The LSM9DS1 sensor chip was selected because it is a representative example of a low-cost consumer grade sensor.

---

[1]Since the object is supposed to be still and in a constant, uniform magnetic field, the TRIAD method can be applied for every sensors' sample. However, we use it every 5 seconds to simulate a real walking scenario.
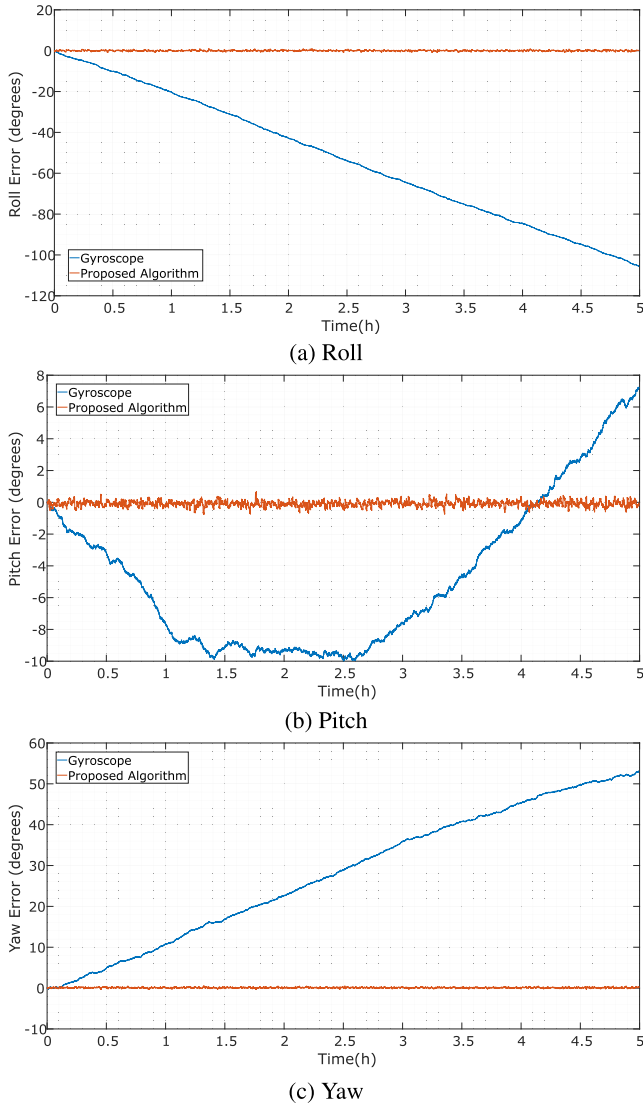
FIGURE 3. Roll (a), pitch (b) and yaw (c) error of the estimated attitude using just the gyroscope's measurements compared to the one using the proposed algorithm.

TABLE 3. Basic performance characteristics of the accelerometer (A), gyroscope (G), and magnetometer (M) included in the LSM9DS1 SiP.

Specification	Value
Measurement Range (A)	$\pm 16g$
Measurement Range (G)	$\pm 2000°/s$
Measurement Range (M)	$\pm 4 Gauss$
Sampling Rate (A, G)	$238 Hz$
Sampling Rate (M)	$80 Hz$
Resolution (A, G, M)	$16 Bits$
*Noise (A)	$226 \mu g/\sqrt{Hz}$
*Noise (G)	$0.017°/s/\sqrt{Hz}$
*Noise (M)	$7.9 \mu T/\sqrt{Hz}$
*Bias Instability (A)	$182 \mu g/h$
*Bias Instability (G)	$8.63°/h$
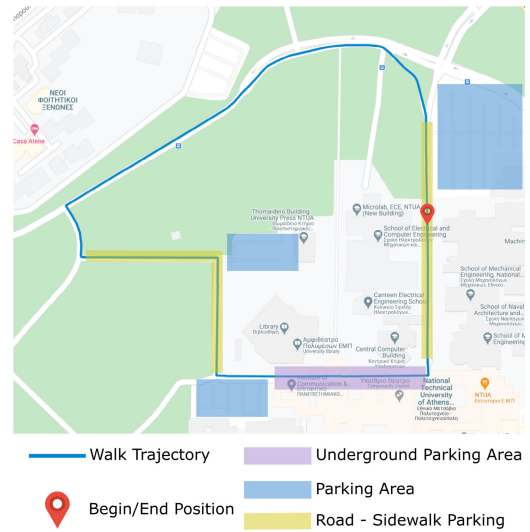
FIGURE 4. Walk path inside the campus of the National Technical University of Athens, Greece.
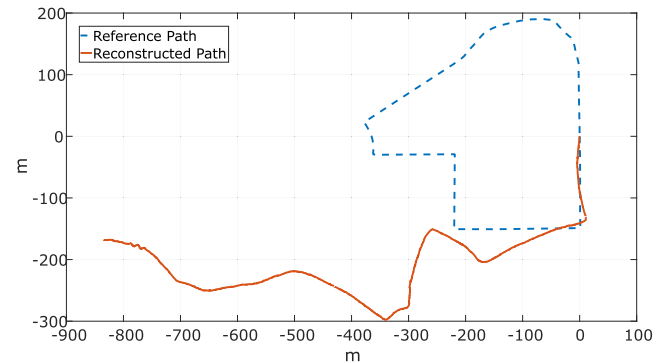
FIGURE 5. Reconstructed walk path using accelerometer and gyroscope measurements and the zero velocity update method.

Some significant performance specifications of the IMU are presented in Table 3. Similar to the case of many commercial low-cost sensors, its noise and bias instability characteristics are not announced by the manufacturer. Thus we use several hours of sensors' measurements and employed the Allan variance [32], [33] to calculate the output noise density and bias instability of the three sensors. In Table 3 these values are marked with a "*" and indicate the average value of the three axis of each sensor.
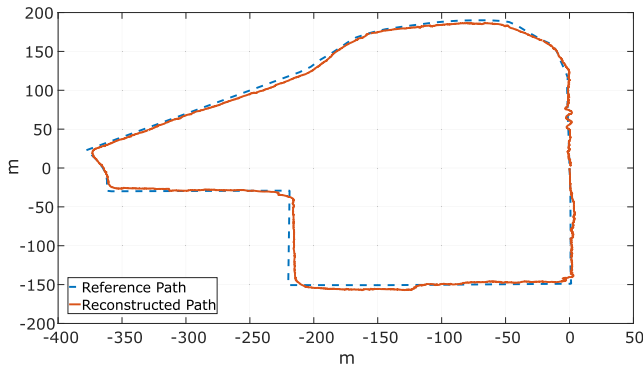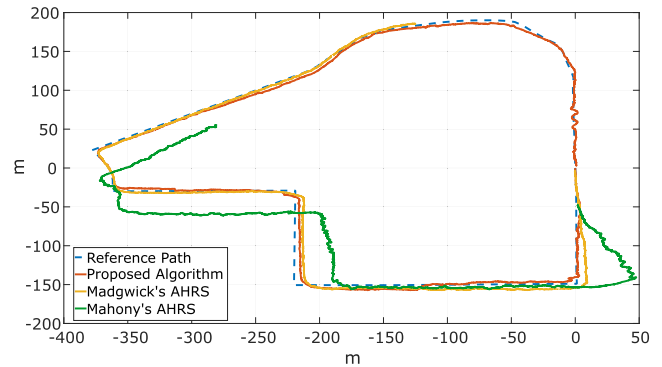
We tested the proposed algorithm by conducting a walk around the campus of the National Technical University of Athens, Greece, which lasted for 20 minutes and covered a distance of approximately 1.3 km. Figure 4 shows the walk path, including important landmarks. The path includes several sources of magnetic disturbance, such as buildings and parking areas.
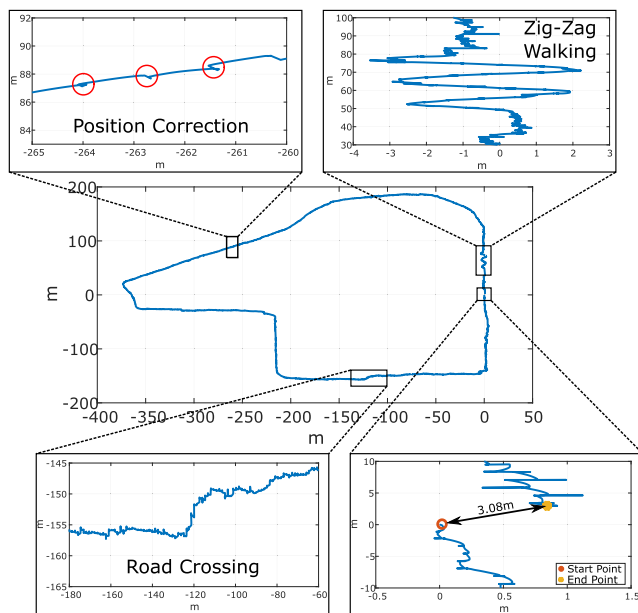
Initially, we demonstrate the long-term accuracy of the proposed system by comparing it to existing pedestrian navigation systems that solely utilize the zero velocity update method. We reconstructed the walk path using only the

FIGURE 6. Reconstructed walk path using the measurements of both inertial and magnetic sensors, the zero velocity update method, and the proposed attitude correction scheme.

FIGURE 8. Reconstructed walk path using the measurements of both inertial and magnetic sensors, the zero velocity update method, and the proposed attitude correction scheme.

demonstrates this by easily identifying a road crossing and a zig-zag pattern while walking. A closer inspection of the reconstructed trajectory reveals the position correction introduced by both the attitude correction scheme and the zero velocity update method in three consecutive steps.

We compared the proposed algorithm with existing pedestrian navigation algorithms in terms of accuracy and computational efficiency using two popular, highly cited attitude and heading reference system (AHRS) algorithms. We combined the zero velocity update method, as described in [16], with Madgwick's AHRS [18] and Mahony's AHRS [17] attitude estimation algorithms similar to [34]. We reconstructed the walking path shown in Figure 4 using the three algorithms.

Figure 8 provides a comparison of the three algorithms in terms of accuracy and long-term stability. The proposed algorithm outperforms both the Madgwick's AHRS and Mahony's AHRS based algorithms, as it successfully tracks the reference path throughout the entire walking distance. The algorithm based on Madgwick's AHRS accurately tracks the reference path and experiences slight drift only during the last 250m, while the Mahony's AHRS based algorithm appears to be less resilient to the magnetic disturbances along the walking path.

Table 4 presents a comparison of the three algorithms in terms of computational efficiency. We executed the three algorithms in MATLAB on a typical quad-core, 8GB RAM PC. Since all three algorithms are based on the same Kalman filter framework to implement the zero velocity update method, the computational burden primarily stems from the attitude estimation algorithm. To ensure a fairer comparison, we executed each algorithm five times using the same dataset,

FIGURE 7. Reconstructed walk path with highlighted important accuracy characteristics.

accelerometer and gyroscope measurements along with the zero velocity update method. As depicted in Figure 5, the calculated attitude drifts after a few meters, and the reconstructed walk path significantly deviates from the reference path.

Figure 6 illustrates the reconstructed walk path using measurements from all three sensors along with the proposed algorithm. It is evident that the reconstructed path successfully tracks the reference path in the long term.

Figure 7 highlights certain accuracy characteristics along the reconstructed path:

The actual path forms a closed loop, starting and ending at exactly the same point. As shown in Figure 7, the reconstructed path exhibits an error of $3.08m$ from the starting point to the ending point. This performance is impressive, as the error is below 0.25% of the total walking distance. The high refresh rate and measurement accuracy of the proposed system enable the identification of walking patterns. Figure 7

TABLE 4. Mean execution time of the proposed algorithm compared to the mean execution time of the algorithms based on Madgwick's AHRS and Mahony's AHRS.

Algorithm	Mean Execution Time
Proposed	$10.67s$
[16] + Madgwick's AHRS [18]	$19.96s$
[16] + Mahony's AHRS [17]	18.32

and the mean execution time of all algorithms is presented in Table 4.

IV. CONCLUSION

This work presented a long-term accurate pedestrian navigation algorithm utilizing low-cost inertial and magnetic field sensors. To address the gyroscope's residual calibration errors and offset drift, a novel approach for attitude correction was introduced, combining the measurements of a three-axis magnetometer and a three-axis accelerometer. Simulation and experimental results demonstrated that the proposed algorithm greatly improves the long-term navigation accuracy compared to using the standard zero velocity update method alone.

APPENDIX A
TRIAD ALGORITHM

Assume two pairs of 3×1 unit vectors, (a_1, b_1) and $(a_2 = Ra_1, b_2 = Rb_1)$ where $R \in SO(3)$, TRIAD algorithm derives R. To this end, it begins by constructing two triads of orthonormal vectors as follows

$$c_1 = a_1, \quad c_2 = (a_1 \times b_1) / \|a_1 \times b_1\|$$
$$c_3 = (a_1 \times (a_1 \times b_1)) / \|a_1 \times b_1\|$$

and

$$d_1 = a_2, \quad d_2 = (a_2 \times b_2) / \|a_2 \times b_2\|$$
$$d_3 = (a_2 \times (a_2 \times b_2)) / \|a_2 \times b_2\|$$

Then, R is derived as

$$R = [d_1 \; d_2 \; d_3] [c_1 \; c_2 \; c_3]^T$$

REFERENCES

[1] A. R. Jiménez, F. Seco, J. C. Prieto, and J. Guevara, "Indoor pedestrian navigation using an INS/EKF framework for yaw drift reduction and a foot-mounted IMU," in *Proc. 7th Workshop Positioning, Navigat. Commun.*, Mar. 2010, pp. 135–143.

[2] C. Fischer, P. T. Sukumar, and M. Hazas, "Tutorial: Implementing a pedestrian tracker using inertial sensors," *IEEE Pervasive Comput.*, vol. 12, no. 2, pp. 17–27, Apr. 2013.

[3] E. Foxlin, "Pedestrian tracking with shoe-mounted inertial sensors," *IEEE Comput. Graph. Appl.*, vol. 25, no. 6, pp. 38–46, Nov. 2005.

[4] Ö. Bebek, M. A. Suster, S. Rajgopal, M. J. Fu, and X. Huang, "Personal navigation via high-resolution gait-corrected inertial measurement units," *IEEE Trans. Instrum. Meas.*, vol. 59, no. 11, pp. 3018–3027, Nov. 2010.

[5] J.-O. Nilsson, A. K. Gupta, and P. Händel, "Foot-mounted inertial navigation made easy," in *Proc. Int. Conf. Indoor Positioning Indoor Navigat. (IPIN)*, Oct. 2014, pp. 24–29.

[6] R. F. Alonso, E. Z. Casanova, and J. G. García-Bermejo, "Pedestrian tracking using inertial sensors," *J. Phys. Agents (JoPha)*, vol. 3, no. 1, pp. 35–43, 2009.

[7] A. R. Jimenez, F. Seco, C. Prieto, and J. Guevara, "A comparison of pedestrian dead-reckoning algorithms using a low-cost MEMS IMU," in *Proc. IEEE Int. Symp. Intell. Signal Process.*, Aug. 2009, pp. 37–42.

[8] R. Jirawimut, P. Ptasinski, V. Garaj, F. Cecelja, and W. Balachandran, "A method for dead reckoning parameter correction in pedestrian navigation system," in *Proc. 18th IEEE Instrum. Meas. Technol. Conf. Rediscovering Meas. Age Informat. (IMTC)*, vol. 3, May 2001, pp. 1554–1558.

[9] R. Stirling, J. Collin, K. Fyfe, and G. Lachapelle, "An innovative shoe-mounted pedestrian navigation system," in *Proc. Eur. Navigat. Conf. GNSS*, Jan. 2003, pp. 110–115.

[10] H. Guo, M. Uradzinski, H. Yin, and M. Yu, "Indoor positioning based on foot-mounted IMU," *Bull. Polish Acad. Sci. Tech. Sci.*, vol. 63, no. 3, pp. 629–634, Sep. 2015.

[11] S. Y. Cho and C. G. Park, "MEMS based pedestrian navigation system," *J. Navigat.*, vol. 59, no. 1, pp. 135–153, Jan. 2006.

[12] J.-O. Nilsson, D. Zachariah, I. Skog, and P. Händel, "Cooperative localization by dual foot-mounted inertial sensors and inter-agent ranging," *EURASIP J. Adv. Signal Process.*, vol. 2013, no. 1, p. 164, Oct. 2013, doi: 10.1186/1687-6180-2013-164.

[13] P. Groves, G. Pulford, C. Littlefield, D. Nash, and C. Mather, "Inertial navigation versus pedestrian dead reckoning: Optimizing the integration," in *Proc. 20th Int. Tech. Meeting Satell. Division Inst. Navigat. (ION GNSS)* vol. 2, Sep. 2007, pp. 2043–2055.

[14] J. Bird and D. Arden, "Indoor navigation with foot-mounted strapdown inertial navigation and magnetic sensors [emerging opportunities for localization and tracking]," *IEEE Wireless Commun.*, vol. 18, no. 2, pp. 28–35, Apr. 2011.

[15] K. Papafotis and P. P. Sotiriadis, "Exploring the importance of sensors' calibration in inertial navigation systems," in *Proc. IEEE Int. Symp. Circuits Syst. (ISCAS)*, Oct. 2020, pp. 1–4.

[16] P. D. Groves, *Principles of GNSS, Inertial, and Multisensor Integrated Navigation Systems*. Norwood, MA, USA: Artech House, 2013.

[17] R. Mahony, T. Hamel, and J.-M. Pflimlin, "Nonlinear complementary filters on the special orthogonal group," *IEEE Trans. Autom. Control*, vol. 53, no. 5, pp. 1203–1218, Jun. 2008.

[18] S. O. H. Madgwick, A. J. L. Harrison, and R. Vaidyanathan, "Estimation of IMU and MARG orientation using a gradient descent algorithm," in *Proc. IEEE Int. Conf. Rehabil. Robot.*, Jun. 2011, pp. 1–7.

[19] H. Fourati, "Heterogeneous data fusion algorithm for pedestrian navigation via foot-mounted inertial measurement unit and complementary filter," *IEEE Trans. Instrum. Meas.*, vol. 64, no. 1, pp. 221–229, Jan. 2015.

[20] V. Renaudin, M. H. Afzal, and G. Lachapelle, "New method for magnetometers based orientation estimation," in *Proc. IEEE/ION Position, Location Navigat. Symp.*, May 2010, pp. 348–356.

[21] D. Choukroun, I. Y. Bar-Itzhack, and Y. Oshman, "Novel quaternion Kalman filter," *IEEE Trans. Aerosp. Electron. Syst.*, vol. 42, no. 1, pp. 174–190, Jan. 2006.

[22] P. Martin and E. Salaün, "Design and implementation of a low-cost observer-based attitude and heading reference system," *Control Eng. Pract.*, vol. 18, no. 7, pp. 712–722, Jul. 2010. [Online]. Available: https://www.sciencedirect.com/science/article/pii/S0967066110000201

[23] V. Renaudin and C. Combettes, "Magnetic, acceleration fields and gyroscope quaternion (MAGYQ)-based attitude estimation with smartphone sensors for indoor pedestrian navigation," *Sensors*, vol. 14, no. 12, pp. 22864–22890, Dec. 2014. [Online]. Available: https://www.mdpi.com/1424-8220/14/12/22864

[24] K. Papafotis, "Inertial and magnetic sensors: Calibration and data fusion with application to navigation," Ph.D. thesis, School Elect. Comput. Eng., Nat. Tech. Univ. Athens, Athens, Greece, Jun. 2022.

[25] K. Papafotis and P. P. Sotiriadis, "MAG.I.C.AL.—A unified methodology for magnetic and inertial sensors calibration and alignment," *IEEE Sensors J.*, vol. 19, no. 18, pp. 8241–8251, Sep. 2019.

[26] P. G. Savage, *Strapdown Analytics, Part 2*. Independence, MN, USA: Strapdown Associates, 2007.

[27] I. Skog, P. Handel, J. O. Nilsson, and J. Rantakokko, "Zero-velocity detection—An algorithm evaluation," *IEEE Trans. Biomed. Eng.*, vol. 57, no. 11, pp. 2657–2666, Nov. 2010.

[28] Z. Wang, H. Zhao, S. Qiu, and Q. Gao, "Stance-phase detection for ZUPT-aided foot-mounted pedestrian navigation system," *IEEE/ASME Trans. Mechatronics*, vol. 20, no. 6, pp. 3170–3181, Dec. 2015.

[29] H. D. Black, "A passive system for determining the attitude of a satellite," *AIAA J.*, vol. 2, no. 7, pp. 1350–1351, Jul. 1964, doi: 10.2514/3.2555.

[30] M. D. Shuster and S. D. Oh, "Three-axis attitude determination from vector observations," *J. Guid. Control*, vol. 4, no. 1, pp. 70–77, Jan. 1981, doi: 10.2514/3.19717.

[31] L. M. Ryzhkov, M. V. Ozhoh, and O. V. Prokopovych, "Analysis of attitude determination algorithm TRIAD errors," in *Proc. IEEE 3rd Int. Conf. Methods Syst. Navigat. Motion Control (MSNMC)*, 2014, pp. 176–181, doi: 10.1109/MSNMC.2014.6979763.

[32] D. W. Allan, "Statistics of atomic frequency standards," *Proc. IEEE*, vol. 54, no. 2, pp. 221–230, Feb. 1966.

[33] N. El-Sheimy, H. Hou, and X. Niu, "Analysis and modeling of inertial sensors using Allan variance," *IEEE Trans. Instrum. Meas.*, vol. 57, no. 1, pp. 140–149, Jan. 2008.

[34] X. Li and Y. Wang, "Evaluation of AHRS algorithms for foot-mounted inertial-based indoor navigation systems," *Open Geosci.*, vol. 11, no. 1, pp. 48–63, Mar. 2019, doi: 10.1515/geo-2019-0005.
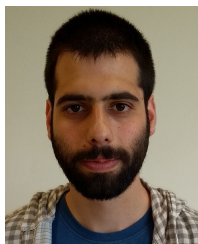
KONSTANTINOS PAPAFOTIS (Member, IEEE) received the Diploma degree in electrical and computer engineering from the National Technical University of Athens, Greece, in 2015, and the Ph.D. degree in electrical and computer engineering under the supervision of Prof. Paul P. Sotiriadis. His Ph.D. thesis is about calibration of inertial and magnetic filed methods and their applications in the field of inertial navigation. His research interests include inertial navigation, embedded systems, and wireless sensors systems. He is the author of several conference papers and journal articles. He has received the Best Paper Award in the IEEE International Conference on Modern Circuits and Systems Technologies, in 2019. He is a regular reviewer for many IEEE publications.

PAUL P. SOTIRIADIS (Fellow, IEEE) received the Diploma degree (Hons.) in electrical and computer engineering from the National Technical University of Athens (NTUA), Greece, in 1994, the M.S. degree in electrical engineering from Stanford University, USA, in 1996, and the Ph.D. degree in electrical engineering and computer science from the Massachusetts Institute of Technology, USA, in 2002.

In 2002, he joined as a Faculty Member of the Electrical and Computer Engineering Department, Johns Hopkins University. In 2012, he joined as a Faculty Member of the Electrical and Computer Engineering Department, NTUA, where he is currently a Professor in electrical and computer engineering and the Director of the Electronics Laboratory. He is also a Governing Board Member of the Hellenic (National) Space Center of Greece. He runs a team of 25 researchers. He has authored and coauthored more than 200 research publications, most of them in IEEE journals and conferences, holds one patent, and has contributed several chapters to technical books. His research interests include the design, optimization, and mathematical modeling of analog, mixed–signal and RF integrated and discrete circuits, sensor and instrumentation architectures with emphasis in biomedical instrumentation, advanced RF frequency synthesis, the application of machine learning and general AI in the operation, and the design of electronic circuits.

Prof. Sotiriadis has received several awards, including the prestigious Guillemin–Cauer Award from the IEEE Circuits and Systems Society, in 2012, the Best Paper Award in the IEEE International Symposium on Circuits and Systems (ISCAS), in 2007, the Best Paper Award in the IEEE International Frequency Control Symposium (IFCS), in 2012, the Best Paper Award in the IEEE International Conference on Modern Circuits and Systems Technologies (MOCAST), in 2019, the Best Paper Award in the IEEE International Conference on Microelectronics (ICM), in 2020 and 2021, the Best Paper Award in the IEEE Symposium on Integrated Circuits and Systems Design (SBCCI), in 2021, the Best Paper Award in the First International Conference on Frontiers of Artificial Intelligence, Ethics, and Multidisciplinary Applications, in 2023, and the IEEE Circuits and Systems Society (CASS) Outstanding Technical Committee Recognition, in 2022. Also, he has been in the list of the top 2% most influential researchers in the world in 2020, 2022, and 2023. He is a member of the IEEE 2023 CAS Fellows Evaluation Committee (FEC). He has been a member of technical committees of many conferences. He regularly reviews for many IEEE TRANSACTIONS and conferences and serves on proposal review panels. He is also an Associate Editor of IEEE SENSORS JOURNAL. He has served as an Associate Editor for IEEE TRANSACTIONS ON CIRCUITS AND SYSTEMS I: REGULAR PAPERS (2016–2020) and IEEE TRANSACTIONS ON CIRCUITS AND SYSTEMS II: EXPRESS BRIEFS (2005–2010).

• • •